Optics Communications 283 (2010) 3081–3088

Contents lists available at ScienceDirect

Optics Communications

journal homepage: www.elsevier.com/locate/optcom

Role of dispersion profile in controlling emission of dispersive waves by solitons in supercontinuum generation

Samudra Roy [a], Debashri Ghosh [a], Shyamal K. Bhadra [a,*], Govind P. Agrawal [b]

[a] Fiber Optics and Photonics Division, Central Glass and Ceramic Research Institute, CSIR 196 Raja S. C. Mullick Road, Kolkata-700032, India
[b] Institute of Optics and Department of Physics and Astronomy, University of Rochester, Rochester, NY, 14627, USA

ARTICLE INFO

Article history:
Received 25 November 2009
Received in revised form 1 April 2010
Accepted 1 April 2010

ABSTRACT

We study the supercontinuum process in optical fibers numerically for a variety of dispersion profiles to investigate how a specific dispersion profile controls the emission of dispersive waves. We conclude that the number of zero-dispersion points in the dispersion profile of a fiber is an excellent predictor of the dispersive-wave peaks when it is pumped with femtosecond pulses in the anomalous dispersion regime. Our study reveals that two or more such peaks can form on the same side of the input wavelength in specially designed and practically achievable dispersion profiles. We show that dispersive waves are emitted even in the case of normal dispersion where soliton fission does not occur. We suggest that a phenomenon related to soliton spectral tunneling is responsible for this radiation. Distinct dispersive peaks may also appear when an optical pulse, launched in the normal dispersion region, later begins to propagate in the anomalous dispersion regime because of its spectral broadening. Several dispersion profiles are numerically employed to show how the soliton fission process creates non-solitonic radiation even under normal dispersion pumping. A time-domain picture clearly shows this radiation when the conventional phase matching condition is satisfied. We also propose a realistic photonic crystal fiber with a dispersion profile that supports dispersive-wave generation in the normal-dispersion region. Our study should prove useful for experiments designed to control the generation of blue light by launching femtosecond pulses into optical fibers.

1. Introduction

Soliton dynamics play a pivotal role in the process of supercontinuum generation occurring when an ultrashort optical pulse is launched in the anomalous-dispersion regime of a nonlinear waveguide such as an optical photonic crystal fiber [1]. In particular, the ideal periodic evolution of a higher-order soliton is perturbed by third- and higher-order dispersions (HOD) to the extent that it breaks into its fundamental components, a phenomenon known as soliton fission [2]. During the fission process, the HOD terms lead to transfer of energy from the soliton to a narrowband resonant dispersive wave (DW), also called non-solitonic radiation [3–5]. This DW is emitted on the blue side of the original pulse spectrum for positive values of third-order dispersion and is of practical importance for generating blue-shifted radiation. The frequency of the DW is accurately determined by a phase-matching condition [4] in the form of a polynomial whose coefficients depend on the numerical values of third, fourth, and other HOD terms. Such a phase-matching condition clearly indicates that dispersion profile plays a dominant role in controlling DWs.

In a recent paper [6] we studied how the individual dispersion coefficients and their numerical signs affect dramatically the formation of DWs. In particular, we concluded that all odd-order dispersion terms produce a single DW, whereas positive even-order dispersion terms produce two DWs. More than two DWs can also be generated for a suitable choice of the individual dispersion coefficients. We also predicted that no DW is created for negative values of the even-order dispersion terms because the phase-matching condition is then never satisfied.

However, such a study is incomplete because it does not answer the question how a specific set of values for various dispersion coefficients can be realized. In practice, the design details of a specific fiber produce a dispersion profile $\beta_2(\omega)$ that shows how the second-order dispersion β_2 changes with frequency ω (or wavelength). All HOD parameters are determined by this profile as various derivatives of $\beta_2(\omega)$. In this paper we identify specific dispersion profiles and correlate them with generated DWs. Our numerical simulations indicate that the number of zero-dispersion points (ZDPs) present in a specific dispersion profile is an excellent predictor of the number of DW peaks created in the supercontinuum produced at the fiber output.

Another interesting feature we find is that, if the frequency of the ZDP is larger (smaller) compare to the operating frequency, DWs always fall on the higher (lower) frequency side of the carrier frequency.

* Corresponding author.
E-mail address: skbhadra@cgcri.res.in (S.K. Bhadra).

0030-4018/$ – see front matter © 2010 Elsevier B.V. All rights reserved.
doi:10.1016/j.optcom.2010.04.003

Therefore there is a possibility to generate two DW peaks on same side (blue or red side) of the output pulse spectrum by tailoring the dispersion curve suitably such that two ZDPs fall on the same side of input frequency. We study a variety of dispersion profiles and their impact on DW generation in detail. Finally we show that DWs can be generated for specific dispersion profiles even when input pulse is launched in the normal-dispersion region of a fiber. Soliton spectral tunneling is an essential phenomenon that takes places simultaneously during the generation of DW in the case of normal dispersion. We propose a specific design of a photonic crystal fiber (PCF) that supports the generation of dispersive waves even when the input pulse is launched in the normal dispersion regime.

2. Theoretical details

Generally a dispersive wave is not phased-matched with a soliton because the soliton's wave number lies in a range forbidden for a linear DW. The presence of HOD terms, however, leads to a phase-matching situation in which energy is transferred from the soliton to a DW at specific frequencies. In the supercontinuum process, HOD terms act as perturbations that split a Nth order soliton into N fundamental solitons of different widths and amplitudes. The kth order soliton has a width T_k that is $(2N-2k+1)$ times smaller than the input pulse width T_0 and its peak power is larger by a factor of $(2N-2k+1)^2/N^2$ [5]. In a dimensionless notation, the frequencies of DWs can be calculated by using a relatively simple phase-matching condition [6]

$$\sum_{m=2}^{\infty} \delta_m x^m = \frac{1}{2}(2N-1)^2, \tag{1}$$

where $\delta_m = \beta_m/(m!|\beta_2|T_0^{m-2})$, $x = 2\pi(\nu_d - \nu_s)T_0$, and ν_s and ν_d are the carrier frequencies associated with the soliton and the DW, respectively. Here, the mth-order dispersion coefficient is represented by β_m.

The real-valued solutions of the polynomial in Eq. (1) can readily predict the exact frequencies of all DWs. The number of real roots and their frequencies depend critically on the values of dimensionless parameters δ_m and their algebraic signs. It should be mentioned that the Eq. (1) applies only for the shortest soliton with the maximum peak power ($k=1$), which is primarily responsible for generating DWs. Other much wider solitons may produce DWs with negligible energies but these are not considered in this paper.

As mentioned earlier, the group-velocity dispersion (GVD) profile $\beta_2(\omega)$ of a fiber determines the dimensionless parameters δ_m and their algebraic signs. The expansion of the $\beta_2(\omega)$ in a Taylor series around the carrier frequency ν_s can be represented in the following dimensionless form:

$$\delta_2(x) = \frac{1}{2}\mathrm{sgn}(\beta_2(\nu_s)) + \frac{1}{2}\sum_{m=1}^{\infty} \frac{(m+2)!}{m!}\delta_{m+2}x^m, \tag{2}$$

where $x = 2\pi(\nu - \nu_s)T_0$. This expression governs the GVD profile for a given set of HOD coefficients.

Dispersion slope is another important parameter that is related to the third-order (3OD) dispersion β_3 and is proportional to the dimensionless quantity δ_3. In our simulations we capture the effect of δ_3 by using a nonzero value of it together with δ_2 and visualise its effect on the spectral evolution. The frequency dependence of $\delta_3(x)$ can be obtained by taking a derivative of the expression in Eq. (2) and is given by

$$\delta_3(x) = \delta_3(0) + \frac{1}{3!}\sum_{m=1}^{\infty} \frac{(m+3)!}{m!}\delta_{m+3}x^m, \tag{3}$$

where $\delta_3(0)$is its value at the carrier frequency of the input pulse.

To capture the impact of higher-order dispersive effects on the DW generation under realistic conditions, we employ a generalized nonlinear Schrödinger equation (GNLSE) written in a normalized form as follows [7]:

$$\frac{\partial U}{\partial \xi} = \frac{i}{2}\frac{\partial^2 U}{\partial \tau^2} + \sum_{m\geq 3}^{\infty} i^{m+1}\delta_m \frac{\partial^m U}{\partial \tau^m} + iN^2\left(1 + is\frac{\partial}{\partial \tau}\right)\left(U(\xi,\tau)\int_{-\infty}^{\tau} R\left(\tau-\tau'\right)\left|U\left(\xi,\tau'\right)\right|^2 d\tau'\right), \tag{4}$$

where the field amplitude $U(\xi, \tau)$ is normalized such that $U(0, 0) = 1$ and the other dimensionless variables are defined as

$$\xi = \frac{z}{L_D}, \qquad \tau = \frac{t - z/v_g}{T_0}, \qquad N = \sqrt{\gamma P_0 L_D}.$$

Here, P_0 is the peak power of the ultrashort pulse launched into the fiber, $L_D = T_0^2/|\beta_2|$is the dispersion length, γ is the nonlinear parameter of the fiber, and $s = (2\pi\nu_s T_0)^{-1}$ is the self-steepening parameter. The nonlinear response function of the optical fiber has the form [7]

$$R(\tau) = (1-f_R)\delta(\tau) + f_R h_R(\tau), \tag{5}$$

where the first and the second terms correspond to the electronic and Raman responses, respectively, with $f_R = 0.245$. As discussed in Ref. [8], the Raman response function can be expressed in the following form

$$h_R(\tau) = (f_a + f_c)h_a(\tau) + f_b h_b(\tau), \tag{6}$$

where the functions $h_a(\tau)$ and $h_b(\tau)$ are defined as

$$h_a(\tau) = \frac{\tau_1^2 + \tau_2^2}{\tau_1\tau_2^2}\exp\left(-\frac{\tau}{\tau_2}\right)\sin\left(\frac{\tau}{\tau_1}\right), \quad h_b(\tau) = \left(\frac{2\tau_b - \tau}{\tau_b^2}\right)\exp\left(-\frac{\tau}{\tau_b}\right), \tag{7}$$

and the coefficients $f_a = 0.75$, $f_b = 0.21$, and $f_c = 0.04$ quantify the relative contributions of the isotropic and anisotropic parts of the Raman response. In Eq. (5),τ_1, τ_2 and τ_b have values of 12, 32 and 96 fs, respectively. In our notation, they are normalized by the input pulse width T_0.

3. Numerical results

We employ the standard split-step Fourier method [7] to solve the GNLSE numerically and include up to eighth-order dispersion terms ($m = 8$) in our numerical simulations. The input pulse $U(0, t) = \mathrm{sech}(t/T_0)$ is assumed to have $T_0 = 50$ fs (full width at half maximum of about 88 fs) at a carrier wavelength of 835 nm. Its peak power is chosen such that the soliton order N takes the value 2 (3 in case of normal GVD pumping), and the fiber length corresponds to two dispersion lengths (ξ varies from 0 to 2). The physical fiber length depends on the value of β_2 and would be 5 m for $\beta_2 = -1$ ps^2/km. Self-steepening effects are negligible in our simulations because $s < 0.01$ for $T_0 = 50$ fs. Thus, intrapulse Raman scattering is the major higher-order nonlinear process affecting the launched pulse. In order to get a desired dispersion profile, the values of HOD coefficients are chosen judiciously.

3.1. Pumping in the anomalous-dispersion regime

Fig. 1 shows the spectra at the fiber output for four different dispersion profiles, along with the corresponding phase-matching condition in Eq. (1). A noteworthy feature of this figure is that the number of ZDPs predicts the number of DW peaks quite accurately. In Fig. 1(a), no DW is generated because the GVD curve never crosses

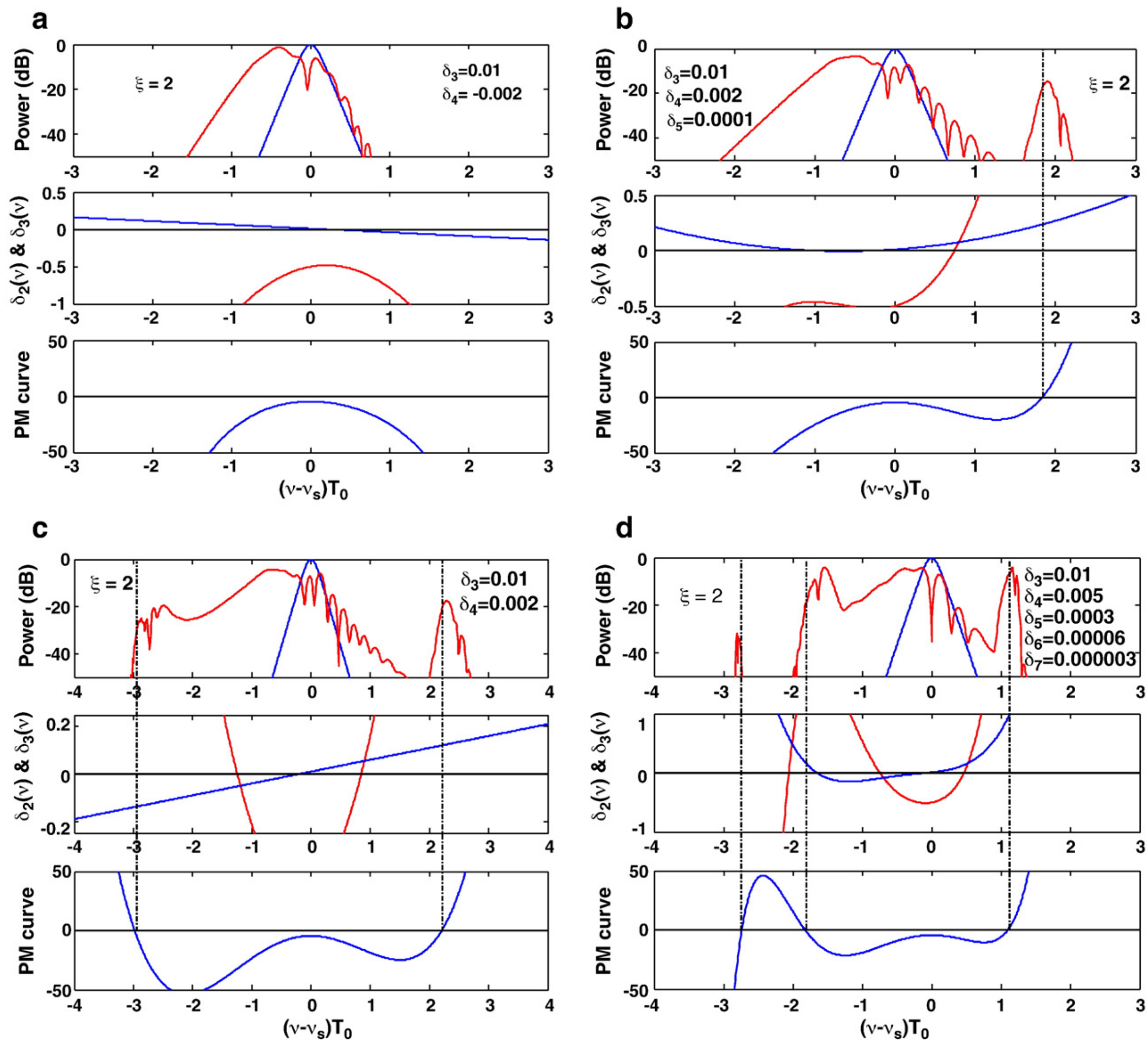

Fig. 1. Formation of DW peaks for four different GVD profiles with (a) no ZDP, (b) single ZDP, (c) two ZDPs, and (d) three ZDPs. In all cases, we show the output spectrum (top), GVD (red line) and dispersion slope (blue line) profiles (middle), and the phase-matching condition (bottom) for a 88-fs pulse propagating as a second-order Soliton ($N = 2$).

the horizontal frequency axis, and the fiber exhibits anomalous dispersion in the entire wavelength range of the output spectrum. We find that this specific situation can only be realized by making the fourth-order and other even-order dispersion coefficients negative. In this case, there is no solution for the phase-matching condition as well.

In Fig. 1(b) we have a dispersion profile with a single ZDP on the high-frequency side of the carrier frequency; we observe a single blue DW peak, as also predicted by the phase-matching condition in Eq. (1). Fig. 1(c) and (d) exhibit two and three ZDPs in the corresponding dispersion profiles, respectively. In both cases, the number of DW peaks matches with the number of ZDPs. A practically useful conclusion that can be drawn from Fig. 1(c) is that, if a microstructured fiber exhibits two zero-dispersion wavelengths, then it will always produce two DW peaks during supercontinuum generation. We verified this conclusion for several combinations of dispersion coefficients that produce two ZDPs and we observed two DW peaks in all cases. It should be mentioned that dispersion profiles with two ZDPs can be realized by using nonzero positive values of even-order dispersion coefficients in the Taylor series expansion in Eq. (2). Also, the results given in Fig. 1(a) and (c) agree well with the experimental observations in Ref [9]. In that paper, dual radiation peaks could only be observed for one specific polarization for which the dispersion profile exhibited two ZDPs. On the other hand, no radiation was observed experimentally for a polarization state for which the dispersion profile did not have any ZDP.

In Fig. 2(a) we create a critical dispersion profile that has four ZDPs, and the corresponding output spectrum exhibits 4 radiation peaks whose location agrees quite well with the phase-matching condition (also plotted in that figure). This special kind of dispersion profile having four ZDPs has recently been proposed by Kibler et al. for studying the soliton-tunneling effect [10]. The proposed structure consists of an air hole of sub-wavelength diameter (about 0.5 μm) in the center of the solid silica core which is surrounded by a standard hexagonal air-hole cladding. Another structure with two sets of different size air-holes has been realized by Poletti et.al. [11] for creating a dispersion profile with three ZDPs. The controlling parameter for such a structure is the inner hole diameter which can be used to tailor the dispersion profile as per the design requirements, while the outer rings reduce the confinement losses. However, the PCF as proposed in Ref. [10] is easier to fabricate because of its structural simplicity.

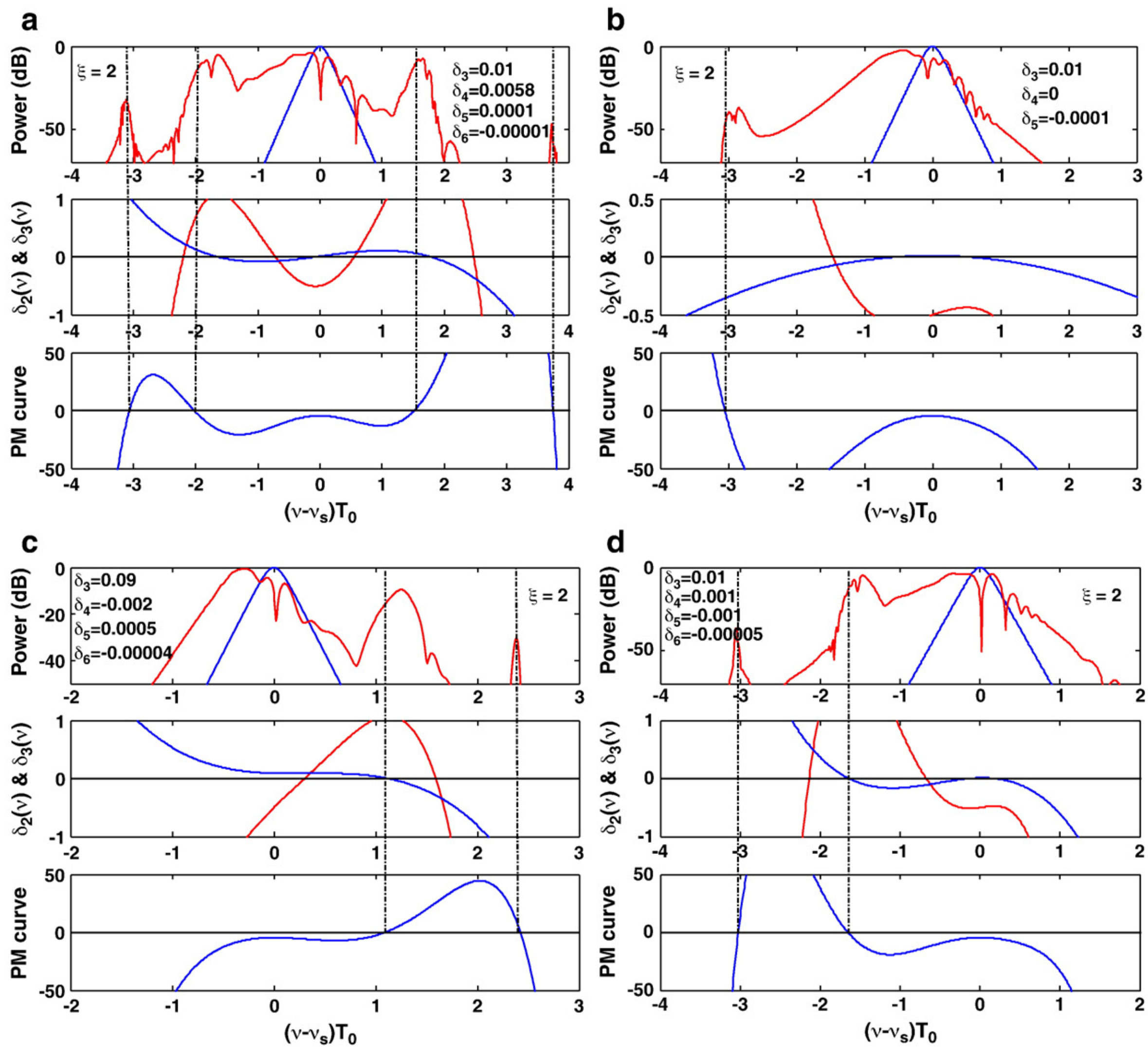

Fig. 2. DW generation under the conditions of Fig. 1 for four specific GVD profiles. Plots (c) and (d) show the cases in which two DW peaks form on the same side of the supercontiunnum.

In all cases of anomalous GVD pumping, the DW frequency follows the frequency of the ZDP in the following sense: if a ZDP falls on the blue (or red) side of the carrier frequency of the input pulse, then the corresponding DW peak also falls on the same side. The expanded polynomial form of Eqs. (1) and (2) can explain this feature mathematically. For a given set of HOD coefficients, the real roots of the two polynomials always maintain the same pattern in terms of their numeric signs. The number of positive and negative roots for both the polynomials are identical, that is, a positive (negative) root of Eq. (1) corresponds to a positive (negative) root of Eq. (2). To verify that this feature is of universal nature, we display in Fig. 2(b) a dispersion profile for which the single ZDP falls on the red side of the input beam. As seen there, the DW peak flips to the red side in this case. The situation in Fig. 2(b) is exactly opposite of what we observe in Fig. 1 (b). To produce such a dispersion profile, we had to use negative values for the odd-order dispersion coefficients in the Taylor series expansion of $\delta_2(x)$ in Eq. (2).

To extrapolate this idea further, we design a special dispersion profile for which two consecutive ZDPs fall on the same side of the carrier frequency. In this case our numerical simulations show that both DW peaks are also generated on the same side. Fig. 2(c) represents the case when the two DW peaks fall on the red side of the input pulse spectrum, whereas Fig. 2(d) shows the opposite case in which two DW peaks fall on the blue side. In both cases, the DW frequencies are accurately identified by the phase-matching condition. To our knowledge, this is the first time that we have shown the possibility of two DW peaks forming on the same side of the input pulse spectrum.

3.2. Pumping in the normal-dispersion regime

Next, we investigate the case when the carrier frequency of the input pulse falls in the normal-dispersion region of the fiber. We consider this situation because solitons normally form only in the anomalous-dispersion regime [2,7], and the phenomenon of soliton fission that plays an important role in the generation of DWs should not occur in the case of normal GVD. In this sense, the investigation of the formation of DWs in case of normal GVD pumping is to some extent unorthodox. In what follows we show that DWs can form in two situations.

Soliton spectral tunneling (SST) is an important mechanism that can generate a DW-type radiation when a soliton tunnels from one anomalous-dispersion region to another one that is separated by an intermediate region of normal dispersion [11,12]. A localized inhomogeneity of GVD is responsible for SST to occur. In our case, the situation is different because we launch a pulse in the normal-dispersion regime. However, the pulse experiences considerable spectral broadening, primarily through self-phase modulation (SPM) which broadens the pulse spectrum symmetrically on both sides of the input spectrum. At some point, a part of the pulse energy enters the anomalous-dispersion region where a soliton can form. The question one may ask is whether the formation of this soliton is accompanied with the emission of some radiation. Our numerical results indicate that this is the case. In Fig. 3 (a) we plot the output spectrum of a femtosecond pulse launched in the normal-dispersion regime of a fiber with $\delta_3 = 0.05$, $\delta_4 = 0.01$ and $\delta_5 = 0.005$ (all other higher-order coefficients set to zero). The spectrum indicates a distinct peak around 1.65 (in normalized unit) that is generated roughly at the same distance into the fiber where a soliton forms with spectrum on the red side. During the SPM process, the pulse spectrum broadens on both sides, but the two sides experience different dispersion regime. The slope of the dispersion (or third-order dispersion) also varies with frequency and influences the spectral behavior as well as the group delay of the pulse. For example, in Fig. 3 (a) the dispersion slope goes from positive to negative roughly at the same point where radiation begins. To ensure the general nature of this observation, we have verified that the same holds true for several different dispersion profiles. This behavior is clearly seen in the middle part of Fig. 3(a). Physically speaking, an abrupt change in the sign of dispersion slope (δ_3 shown by the green curve) perturbs the monotonous broadening of the spectrum and creates a distinct spectral peak on the blue side. This behavior is similar to the soliton tunneling effect but we cannot call it soliton tunneling because most of the pulse energy lies in the normal-dispersion region. It should be noted that the phase-matching condition (shown by a blue curve) does not accurately predict the frequency of this radiation.

After the DW has been generated, a part of the pulse spectrum lies in the anomalous region and can form a soliton. The temporal evolution shown in Fig. 3(b) shows the soliton formation clearly where a part of pulse energy is delayed by a large amount (as much as by 120 T_0). This delay can be understood by noting that the soliton spectrum is shifted towards the red side and that longer wavelengths travel slower in the anomalous-dispersion region.

We have discovered a second mechanism of DW generation. An extensive numerical study, covering a wide range of operating conditions, reveals that DWs can still be generated for a few specific dispersion profiles chosen such that a narrow normal-dispersion region is surrounded on both sides by anomalous regions. In this case, SPM-induced spectral broadening forces most of the pulse

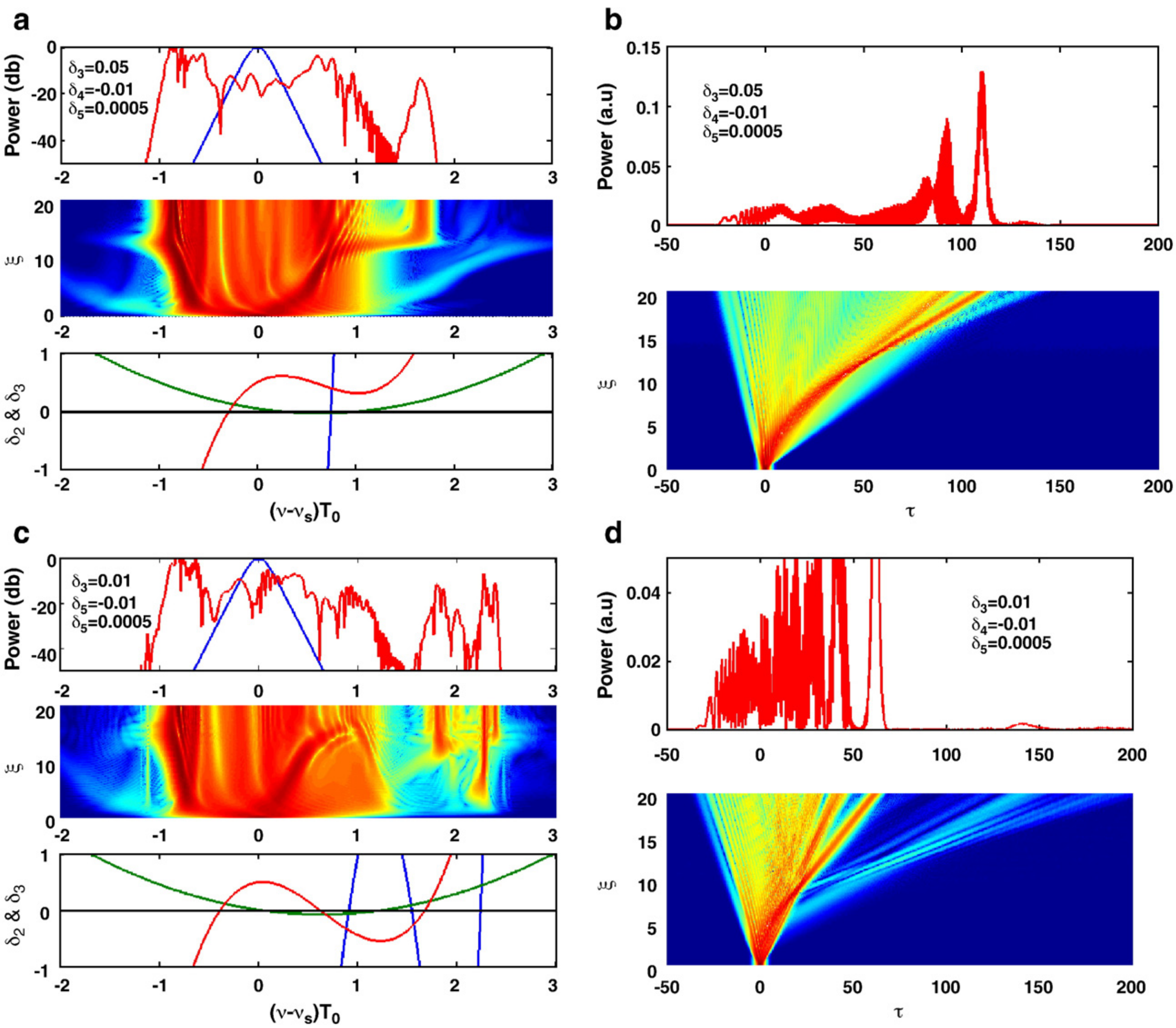

Fig. 3. Spectral tunneling effect under the conditions of Fig. 1 except that the input pulse is launched in the normal-GVD region of the fiber with $N = 3$. (a) Output spectrum (top), spectral evolution (middle) and finally GVD profile (red), dispersion slope (green) and PM expression (blue) of the fiber (bottom) are shown for the parameters $\delta_3 = 0.05$, $\delta_4 = -0.01$ and $\delta_5 = 0.0005$. (b) Output pulse shapes and temporal evolution inside the fiber are depicted when the fiber is pumped at normal GVD domain. Plots (c) and (d) correspond to the different parameters ($\delta_3 = 0.01$, $\delta_4 = -0.01$ and $\delta_5 = 0.0005$) for which DW peak forms on the blue side of the input spectrum. In both the cases third order soliton is used as input.

energy to travel in the anomalous regions as a soliton after some distance along the fiber. After that, a DW can be generated through soliton fission. This situation is illustrated in Fig. 3(c) by changing the dispersion parameters ($\delta_3=0.01$, $\delta_4=0.01$, $\delta_5=0.0005$) from those used for Fig. 3(a) in such a manner that normal-GVD region is surrounded on both sides by anomalous domains (red curve). We now find two distinct spectral peaks at frequencies 1.8 and 2.25 (in normalized units). The peak at 1.8 is due to the tunneling phenomenon discussed earlier. The new peak at 2.25 is due to a DW emitted through soliton fission and satisfies the phase matching condition in Eq. (1). The time domain evolution shown in Fig. 3(d) shows clearly how a DW is emitted near $\xi=10$ with a large blue shift. Because its frequency falls in the normal-dispersion region where blue-shifted components travel slower than the red-shifted ones, this DW is delayed and appears at $\tau\approx 140$ at the output end of the fiber.

The blue-shifted DW peak vanishes when the dispersion parameters of the fiber are changed slightly to $\delta_3=0.01$, $\delta_4=0.01$ and $\delta_5=0.000325$. This case is shown in Fig. 4 (a). For this set of parameters, even though most of the pulse energy eventually enters the anomalous dispersion region, there is no solution of the phase-matching condition that can create a DW (see the blue curve). The time-domain evolution shown in Fig. 4 (b) also supports this argument by exhibiting no trace of a DW radiation. The peak due to the tunneling effect is still observed but its position is now shifted around 1.4 (in normalized units).

In Fig. 4 (c) we manipulate the dispersion curve (red line) in such a manner that it exhibits 3 ZDPs with a narrow anomalous dispersion zone falling on the lower frequency side surrounded by two normal-dispersion zone. For this configuration, we calculate δ_3 (green line) as well as the phase-matching condition (blue line). The phase-matching condition exhibits a DW solution around the normalized frequency of -2.25. The spectral evolution indeed shows such a red-shifted DW peak. The time-domain evolution also shows a DW peak of low amplitude around $\tau=-100$, i.e., DW travels faster than other parts of the pulse. This is understood by noting that the GVD is normal at the DW frequency where red components travel faster than the blue components.

We must emphasize that the traditional phase-matching expression generally fails when optical pulse propagates entirely in normal GVD domain, however, if most of the pulse energy enters the anomalous GVD regime, it can be used to predict the formation of DWs. The tunneling effect, on the other hand, takes place in a concurrent manner that exhibits additional fringes. It can be shown

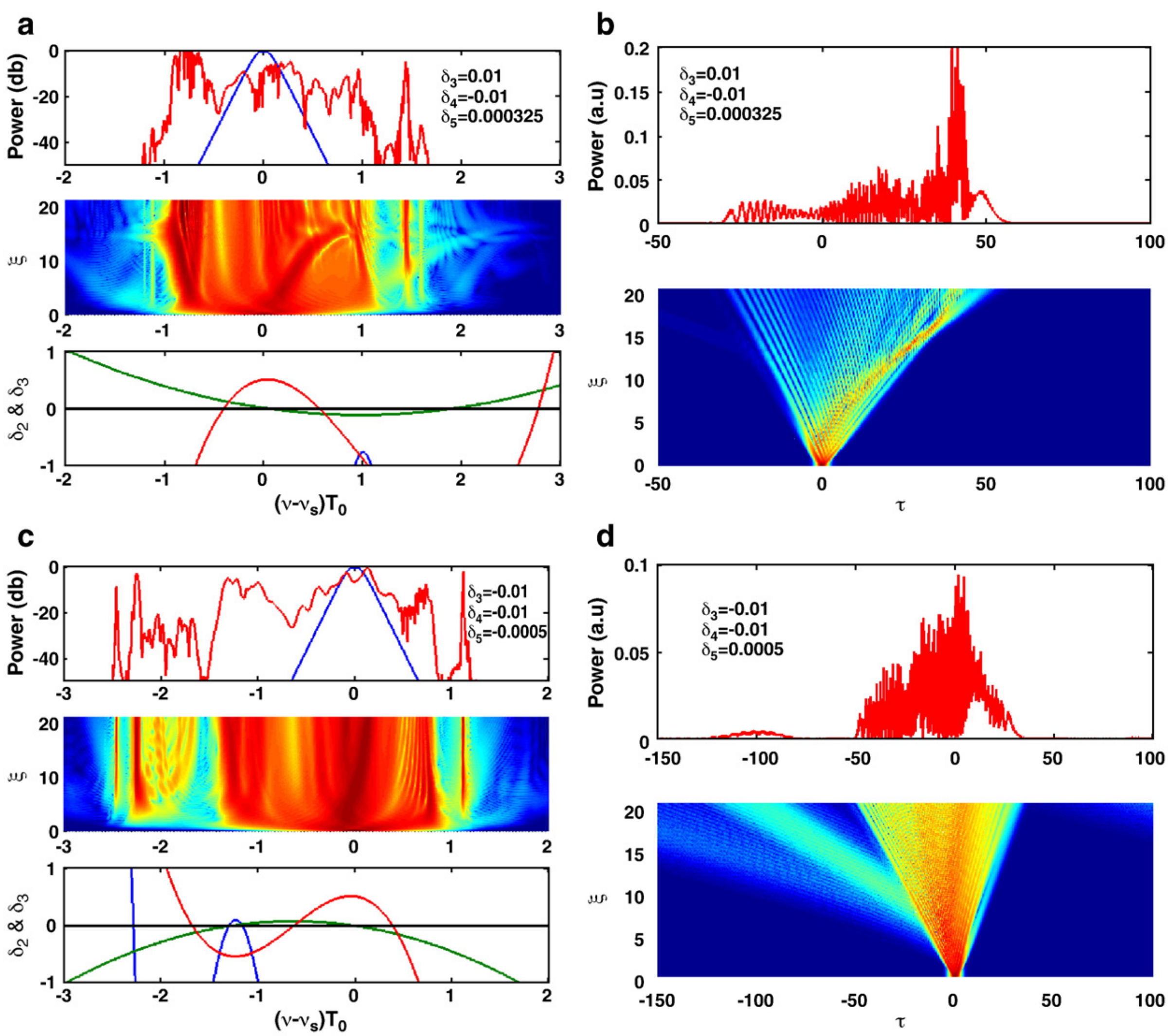

Fig. 4. More different dispersion values are used in order to understand the spectral evolution under normal GVD pumping with soliton order $N=3$. (a) The used parameters are, $\delta_3=0.01$, $\delta_4=-0.01$and $\delta_5=0.000325$. No PM solution can be obtained for those parameters and because of that the generation of DW ceases to exist. (b) Time domain evolution does not exhibit any radiation. (c) The formation of DW in red side is shown for the following normalized dispersion coefficients, $\delta_3=-0.01$, $\delta_4=-0.01$and $\delta_5=-0.0005$. (d) For this case the time domain evolution exhibits the radiation as a pedestal around $\tau\approx-100$ in time domain.

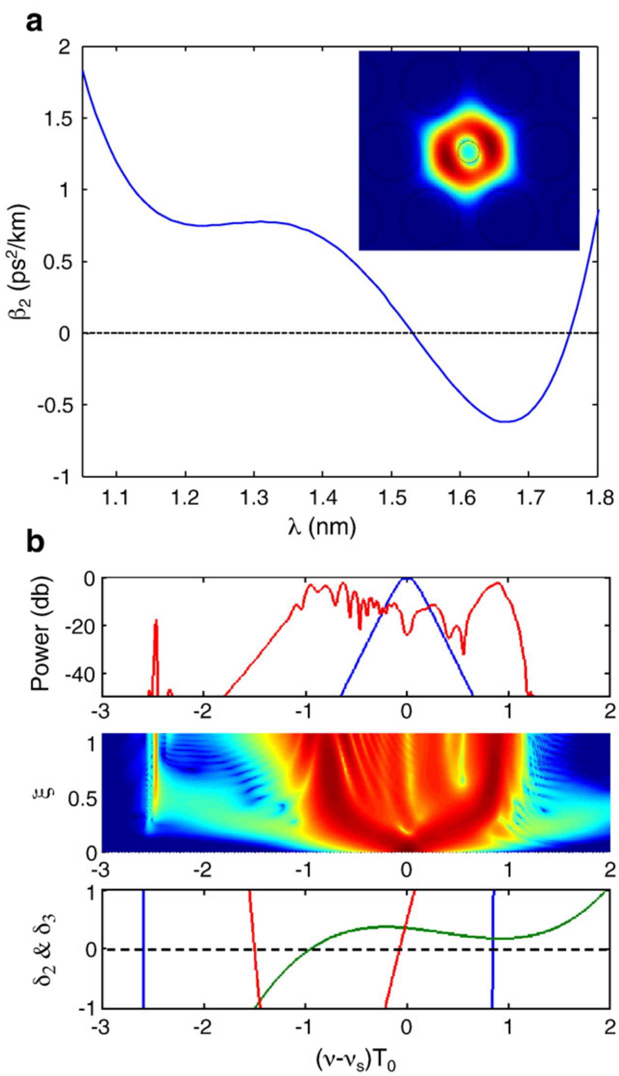

Fig. 5. (a) Dispersion profile of the proposed defect-core PCF having two zero dispersion at 1.531 and 1.760 μm respectively. In the inset the fundamental field distribution at operating wavelength 1.520 μm is depicted for the proposed structure. (b) In panel (b) the dispersive wave radiation is shown around −2.5 normalised frequency which is originated due to the solitonic propagation (for $N=6$) supported by the anomalous dispersion regime as shown by the red line in the bottom figure. The PM condition and evolution of δ_3 is also represented by blue and green curves respectively.

that no such radiation is possible if the GVD profile grows monotonically without any sign change.

In this last part of our study we try to realize a specific dispersion profile with realistic configuration parameters of a PCF that supports the generation of DWs in the normal GVD region of the PCF. We consider a PCF with a sub-wavelength air hole of 0.6 μm in diameter and an air-filling fraction of 0.75 in its cladding containing air holes of 1.5 μm in diameter. It has already been shown that an ultra-flattened dispersion profile can be achieved with such a configuration only by adjusting the size of the central air hole [13]. Fig. 5(a) shows the GVD calculated as a function of wavelength for our proposed structure. As shown in there, we have a reasonable flat dispersion profile having two ZDPs at the wavelengths of 1.531 and 1.760 μm. The dispersion profile is calculated by using the commercial software COMSOL Multiphysics based on the finite-element method. The fundamental modal distribution of the specified structure is given in the inset of Fig. 5 (a).

We next simulate numerically, by solving GNLSE with this dispersion profile, the evolution of the spectrum of a 50-fs pulse launched at 1.52 μm , a wavelength that falls in the normal dispersion regime. Fig. 5(b) shows the output spectrum (top), spectral evolution (middle), and the frequency dependence of dispersion and its slope (red and green curves in the bottom panel). Since the anomalous-dispersion regime is located in the wavelength range of 1.531 to 1.760 μm, the pulse quickly enters the anomalous dispersion zone. A soliton-like propagation can be realized under such conditions and eventually a DW is generated. Interestingly, the phase-matching condition, shown by the blue curve in Fig. 5(b), also predicts a DW around the normalized frequency of −2.5 (in wavelength 2.027 μm), in reasonable agreement with the solution of GNLSE. With further propagation, the red-shifted Raman soliton eventually meets the second ZDP at 1.760 μm and exhibits soliton spectral tunneling phenomenon at that point. The previous studies [4,14] have estimated quantitatively the radiation amplitude as a function of β_3 and soliton order N and concluded that radiation amplitude saturates with increasing values of those two parameters. In the present case, β_3 is the fixed parameter for the given dispersion profile, and we have provided the amplitude of the corresponding DW radiation for a fixed soliton order $N=6$. Since the soliton order is the other important parameter that influences the radiation amplitude, it is expected that radiation efficiency will increase for higher-order solitons with $N>6$ (but not indefinitely).

4. Conclusions

In this paper we have studied numerically the generation of DWs in optical fibers during the supercontinuum process for a variety of dispersion profiles to investigate how a specific dispersion profile controls the emission of DWs. We designed dispersion profiles by using suitable values of the third- and higher-order dispersion coefficients. The most important conclusion is that the number of ZDPs in the dispersion profile of a fiber is an excellent predictor of the DW peaks when an optical pulse is pumped in anomalous GVD regime. We show that a fiber with a single ZDP leads to one DW peak, and a fiber with two ZDPs always produces two DW peaks. Moreover, no DW can be expected in a fiber that has no zero-dispersion crossings over the entire range of wavelengths created during the supercontinuum process. We have examined numerically dispersion profiles with as many as six ZDPs and found that this criterion always holds.

Our study also reveals that two DW peaks can form on the blue or red side of the input carrier frequency through specially designed dispersion profiles with two ZDPs on the same side. The phase-matching condition predicts the DW frequencies accurately when the input pulse is launched in the anomalous-GVD regime of the fiber, but it fails in the case of normal GVD. It is shown that DW peaks are generated even in the case of normal GVD if the pulse enters the anomalous dispersion regime at some distance into the fiber and forms a soliton. We find that a spectral peak can also be generated by a phenomenon related to soliton spectral tunneling. Finally, we propose a realistic design of a PCF that would allow the observation of non-solitonic radiation when pumped with femtosecond pulses in the normal-dispersion region. Our study should prove useful for experiments that are specifically targeted to enhance generation of DWs near the two edges of the super-continuum spectrum generated by launching femtosecond pulses into optical fibers.

Acknowledgements

Authors wish to thank Dr. D.K. Bhattacharya, acting Director, CGCRI, permitting us to publish the paper. Authors (SR) and (DG) are indebted to the Council of Scientific and Industrial Research (CSIR) Govt. of India for financial support in carrying out this work.

References

[1] J.M. Dudley, G. Genty, S. Coen, Rev. Mod. Phys. 78 (2006) 1135.
[2] A. Hasegawa, M. Matsumoto, Optical solitons in fibers, Springer, New York, 2002.
[3] V.I. Karpman, Phys. Rev., E 47 (1993) 2073.
[4] N. Akhmediev, M. Karlsson, Phys. Rev., A 51 (1995) 2602.
[5] A.V. Husakou, J. Herrmann, Phys. Rev. Lett. 87 (2001) 203901.
[6] S. Roy, S.K. Bhadra, G.P. Agrawal, Opt. Lett. 34 (2009) 2072.
[7] G.P. Agrawal, Nonlinear Fiber Optics, 4th ed.Academic Press, Boston, 2007.
[8] Q. Lin, G.P. Agrawal, Opt. Lett. 31 (2006) 3086.
[9] F. Benabid, F. Biancalana, P.S. Light, F. Couny, A. Luiten, P.J. Roberts, J. Peng, A.V. Sokolov, Opt. Lett. 33 (2008) 2680.
[10] B. Kibler, P.A. Lacourt, F. Courvoisier, J.M. Dudley, Electron. Lett. 43 (2007) 967.
[11] F. Poletti, P. Horak, D.J. Richardson, IEEE Photonics Technol. Lett. 20 (2008) 1414.
[12] E.N. Tsoy, C.M. de Sterke, Phys. Rev., A 76 (2007) 043804.
[13] K. Saitoh, N. Florous, M. Koshiba, Opt. Exp. 13 (2005) 8365.
[14] S. Roy, S.K. Bhadra, G.P. Agrawal, Phys. Rev., A 79 (2009) 023824.